Supplementary Material

A comparative study of biradicaloids as ligands in iron tetracarbonyl complexes

M. T. Scharnhölz,[a] P. Coburger,*[a] H. Beer,[b] J. Bresien,[b] A. Schulz,[b,c] and H. Grützmacher[a]

[a] Department of Chemistry and Applied Biosciences, ETH Zürich Vladimir-Prelog-Weg 1, 8093 Zürich, Switzerland

[b] Institut für Chemie, Universität Rostock Albert-Einstein-Str. 3a, 18059 Rostock, Germany

[c] Leibniz-Institut für Katalyse an der Universität Rostock e.V. (LIKAT) Albert-Einstein-Str. 29a, 18059 Rostock, Germany

Email: pcoburger@inorg.chem.ethz.ch hgruetzmacher@ethz.ch

Table of Contents

1. Further synthetic details and spectra of the compounds

1.1 Apparatus for the workup of **2**

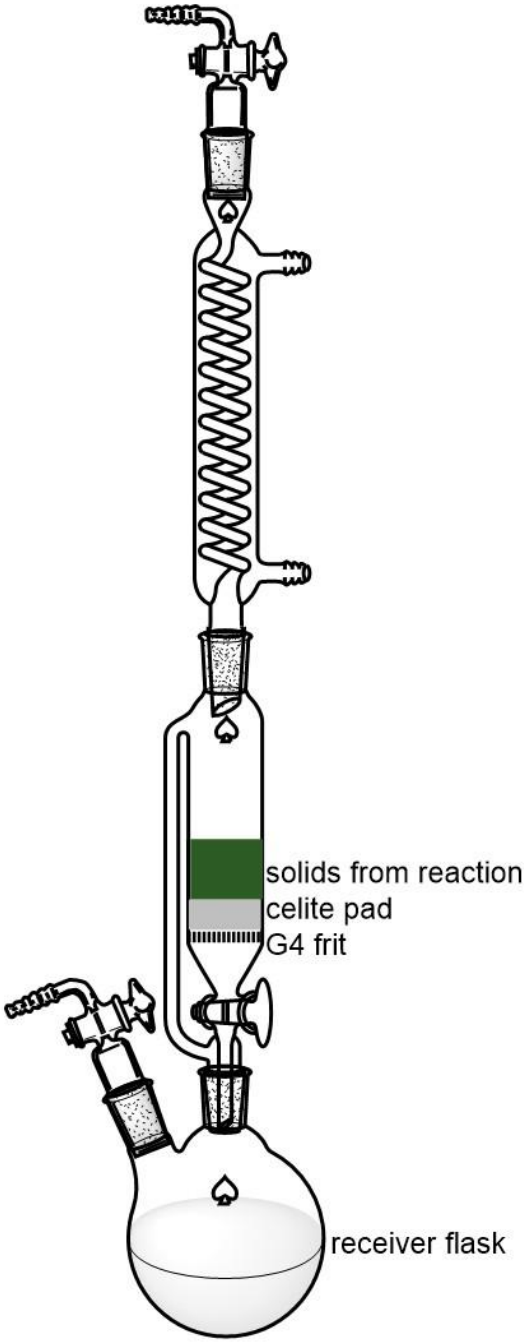

Figure S1: Schematic depiction of the extraction apparatus.

1.2 Spectra of $[Fe(CO)_4\text{-}\{[P(\mu\text{-}NTer)]_2\}]$ (**5**)

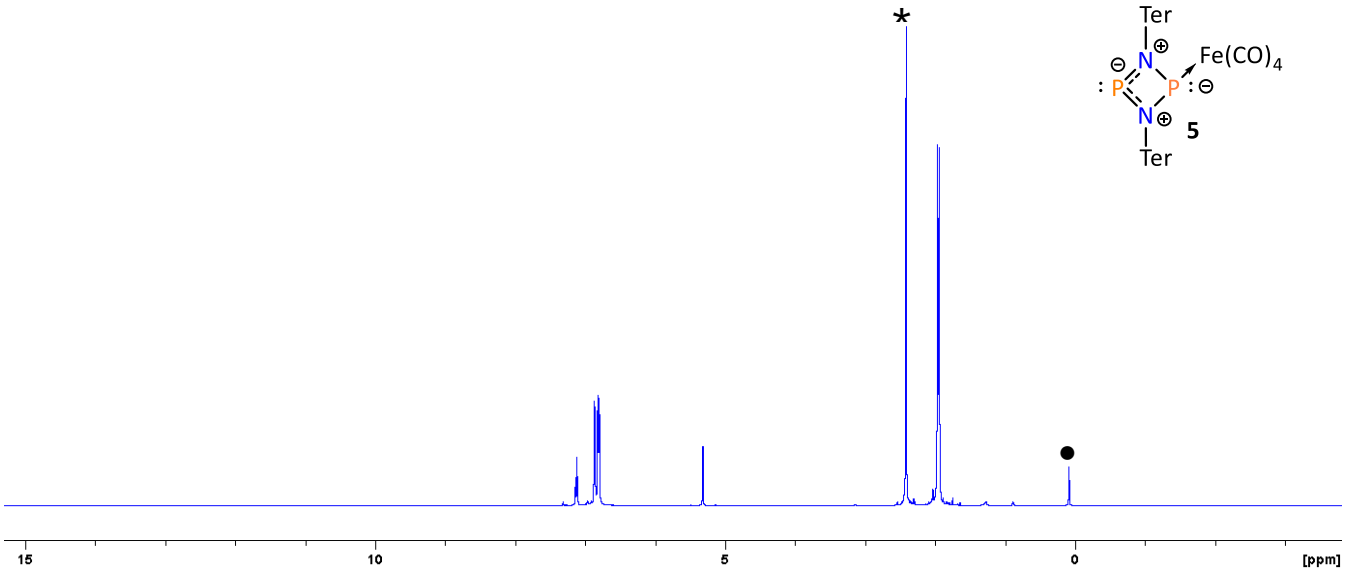

Figure S2: ^{1}H NMR spectrum of **5** at room temperature in CD_2Cl_2. Solvent signal is marked with an asterisk (*). The grease peak is marked with a dot (●).

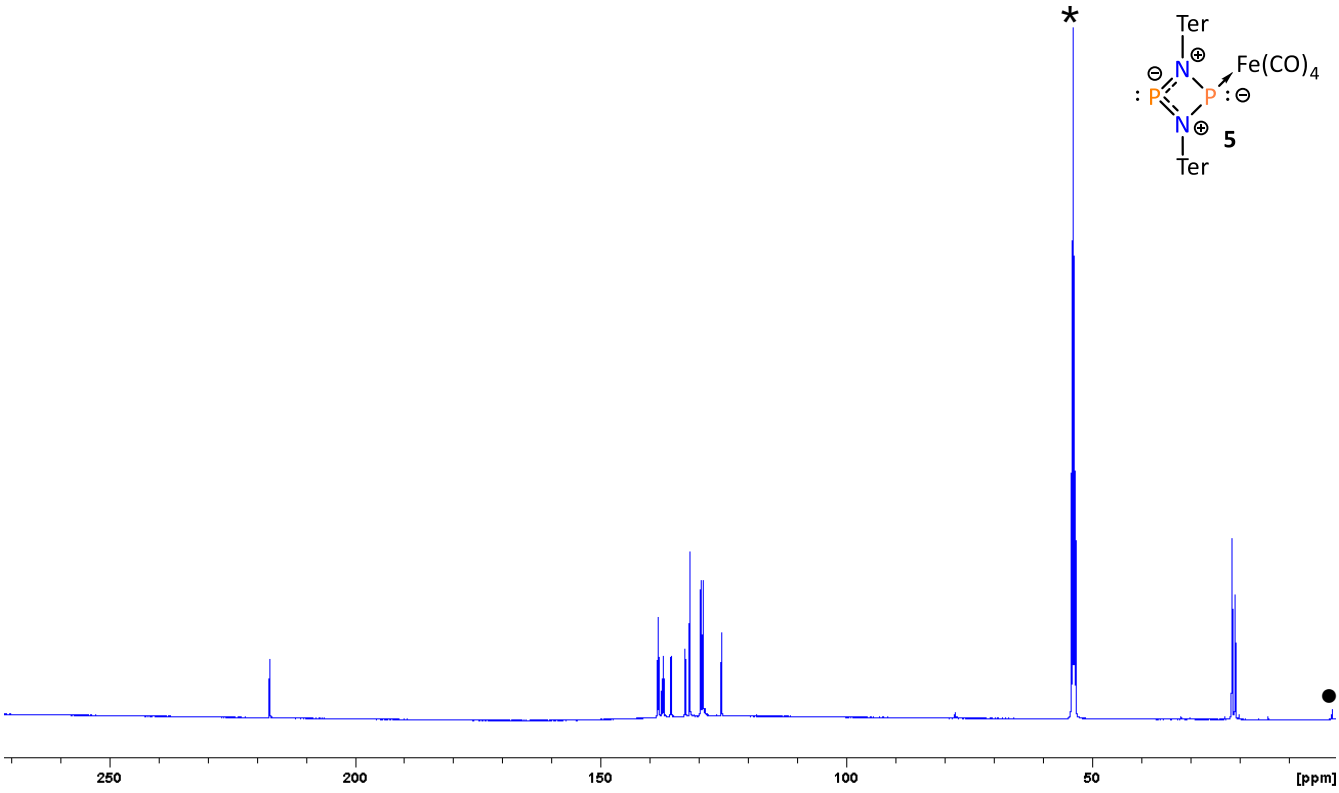

Figure S3: $^{13}C\{^{1}H\}$ NMR spectrum of **5** at room temperature in CD_2Cl_2. Solvent signal is marked with an asterisk (*). The grease peak is marked with a dot (●).

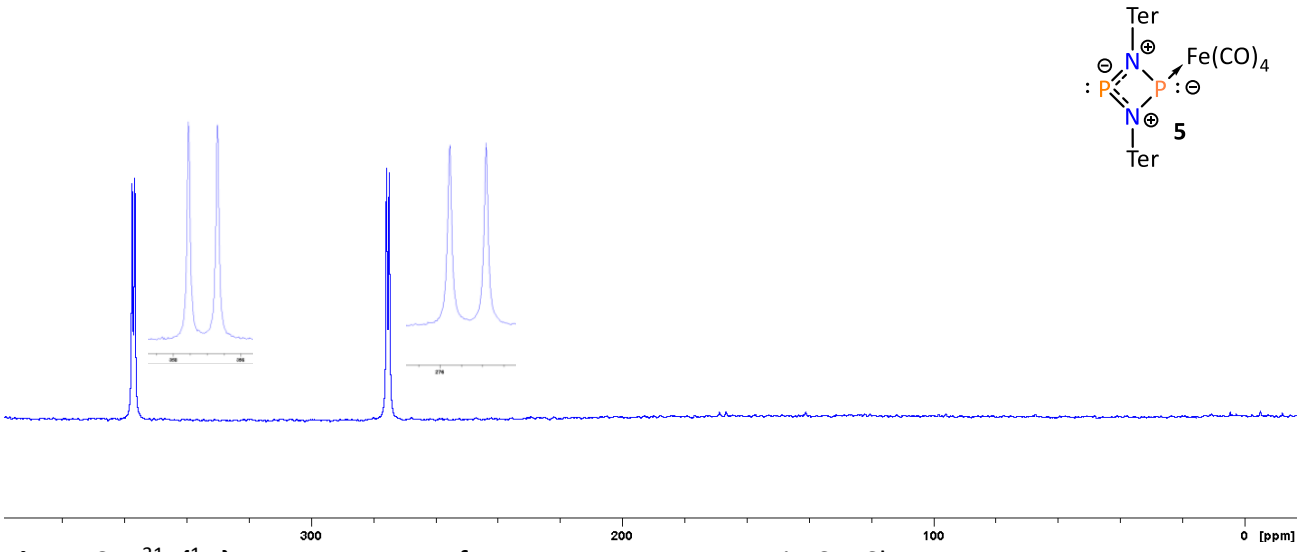

Figure S4: $^{31}P\{^{1}H\}$ NMR spectrum of **5** at room temperature in CD_2Cl_2.

As the signals in ATR-IR were broad in the CO region an additional spectrum was recorded in saturated n-hexane solution.

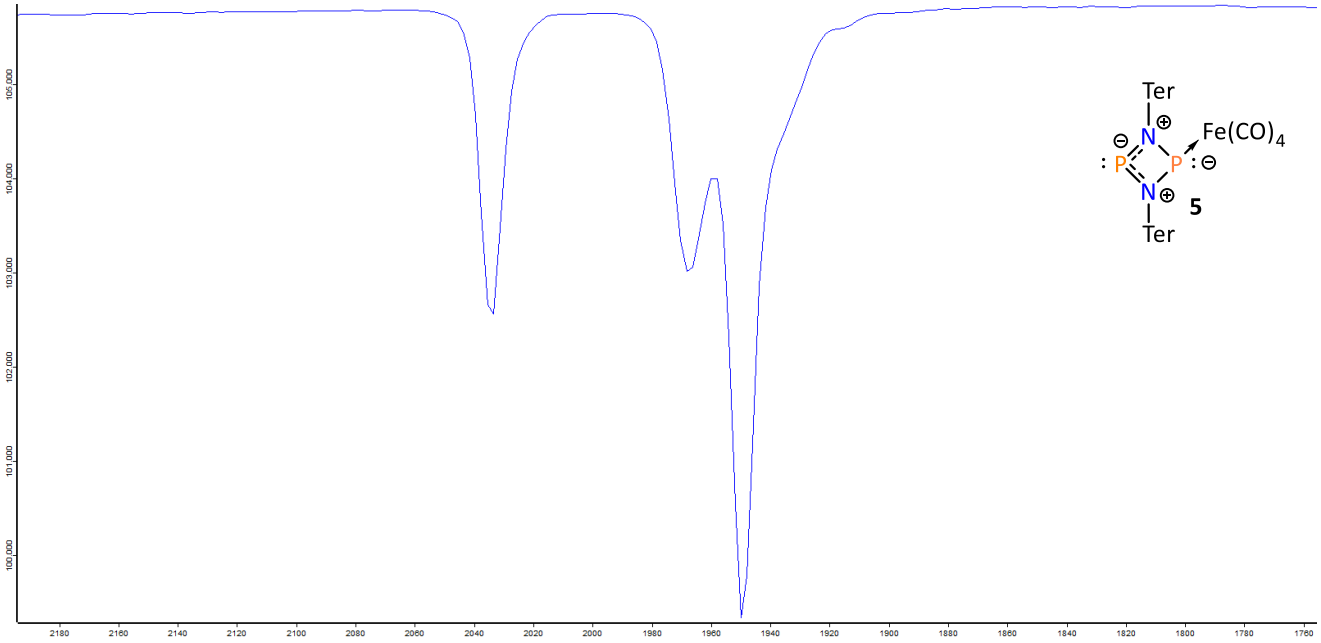

Figure S5: CO-region of the transmission-IR spectrum of **5** at room temperature in saturated n-hexane solution.

1.3 Spectra of [Fe(CO)$_4$-{IDP}] (**6**)

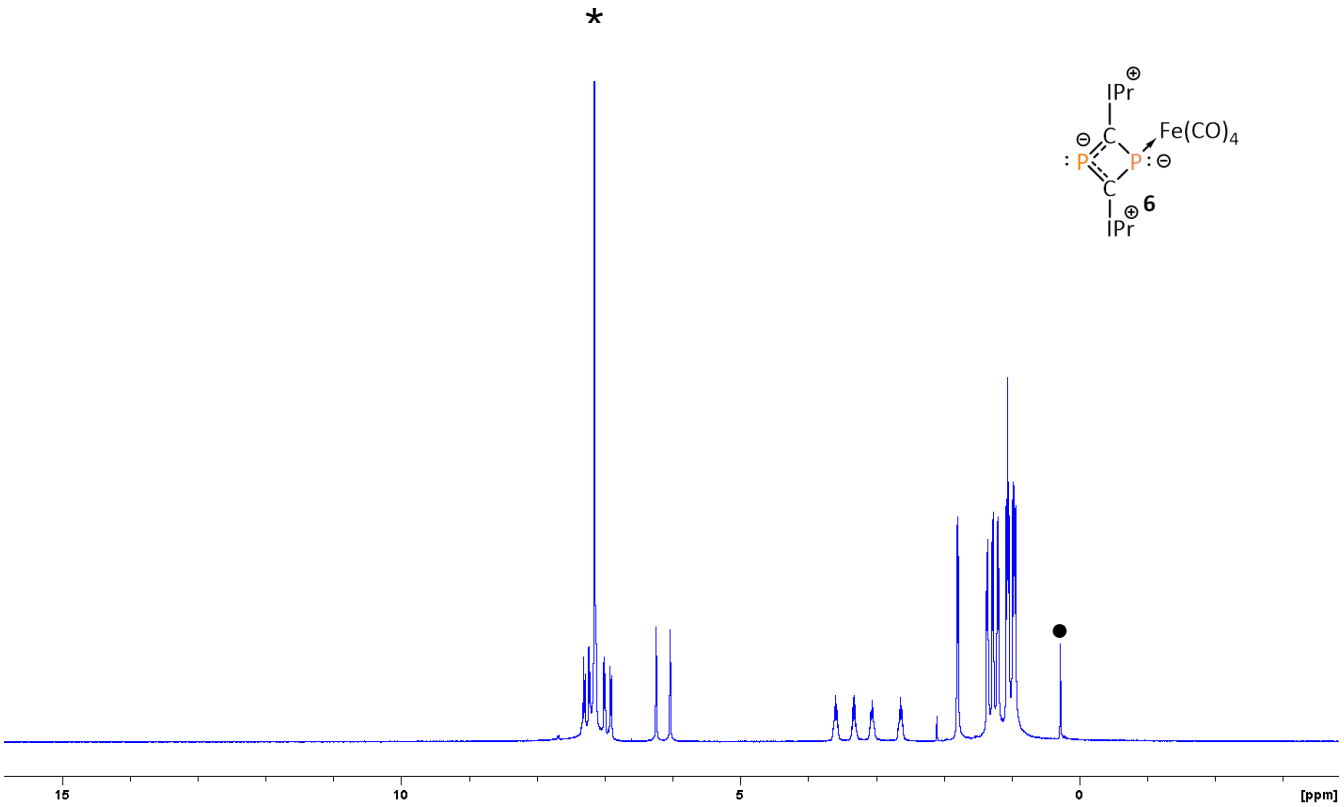

Figure S6: ^{1}H NMR spectrum of **6** at room temperature in C_6D_6. Solvent signal is marked with an asterisk (*). The grease peak is marked with a dot (●).

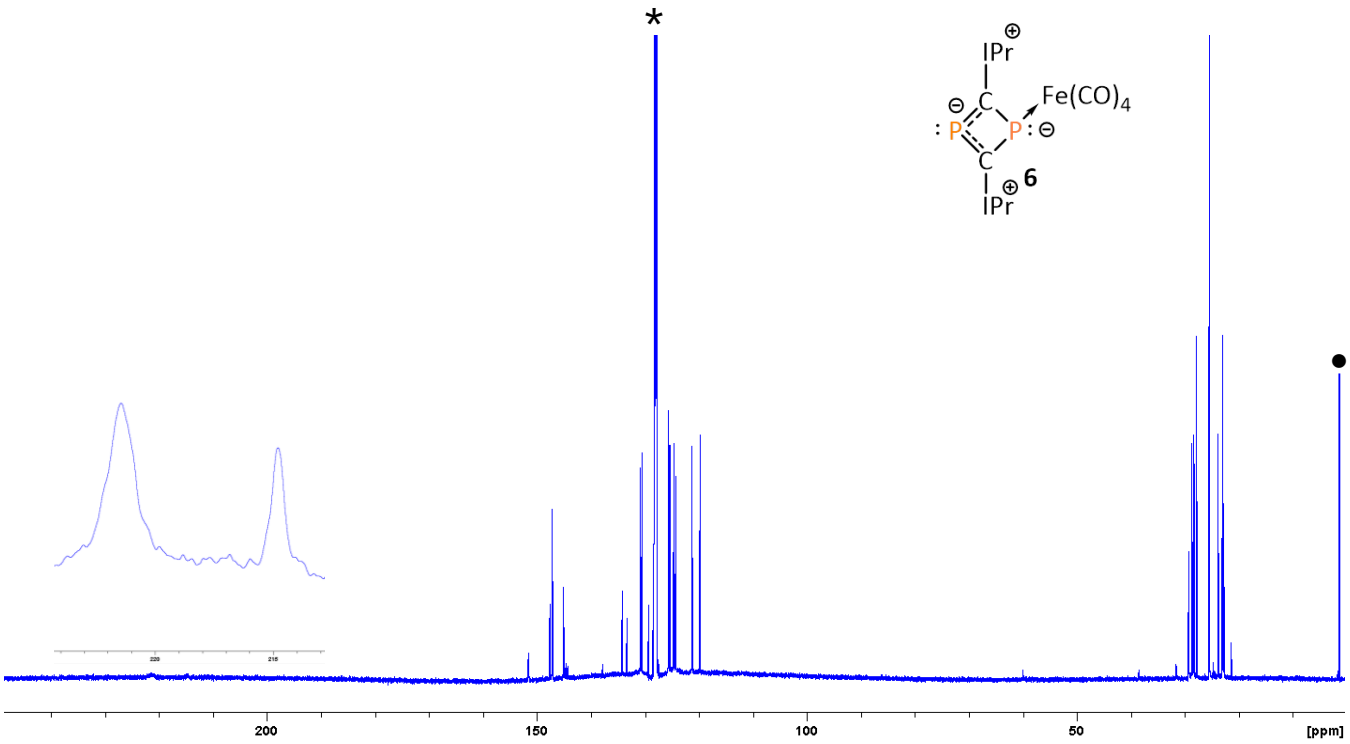

Figure S7: $^{13}C\{^1H\}$ NMR spectrum of **6** at room temperature in C_6D_6. The carbonyl signals at 214.8 ppm and 221.4 ppm are broadened and therefore not resolved in this picture. To the overlayed spectrum a line broadening of 32 Hz was applied, which resolves the carbonyl signals. The solvent signal is marked with an asterisk (*). The grease peak is marked with a dot (●).

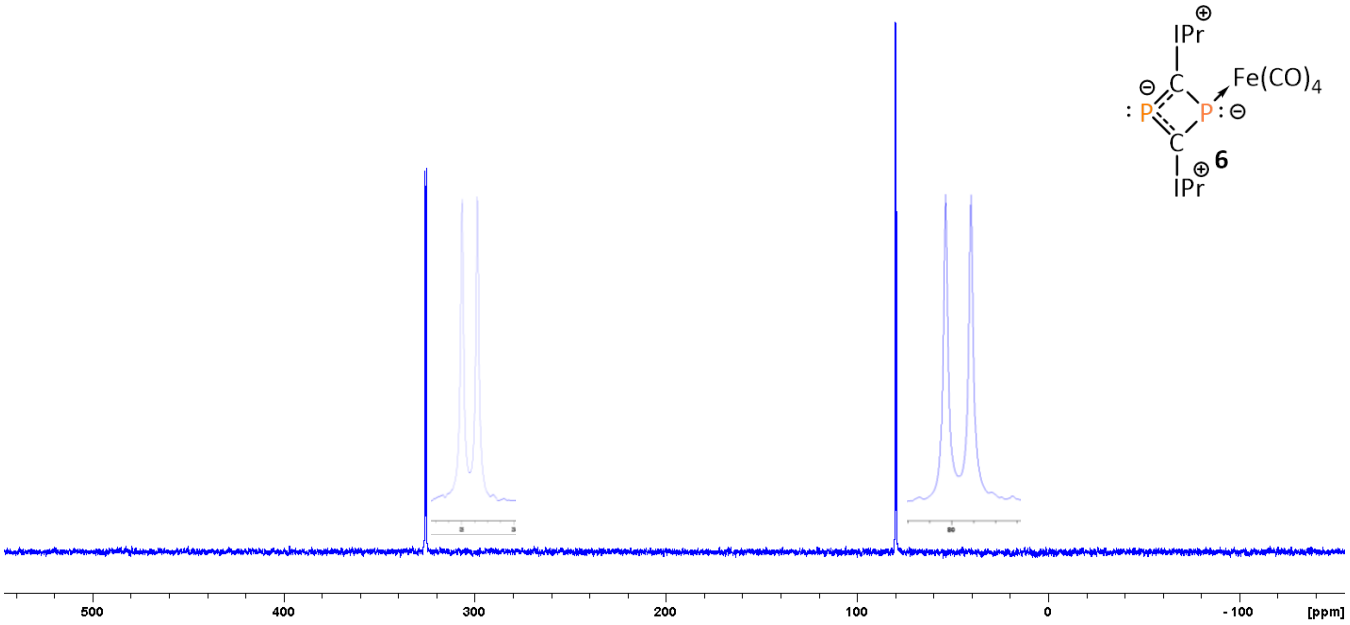

Figure S8: $^{31}P\{^{1}H\}$ NMR spectrum of **6** at room temperature in C_6D_6.

As the signals in ATR-IR were broad in the CO region an additional spectrum was recorded in saturated n-hexane solution.

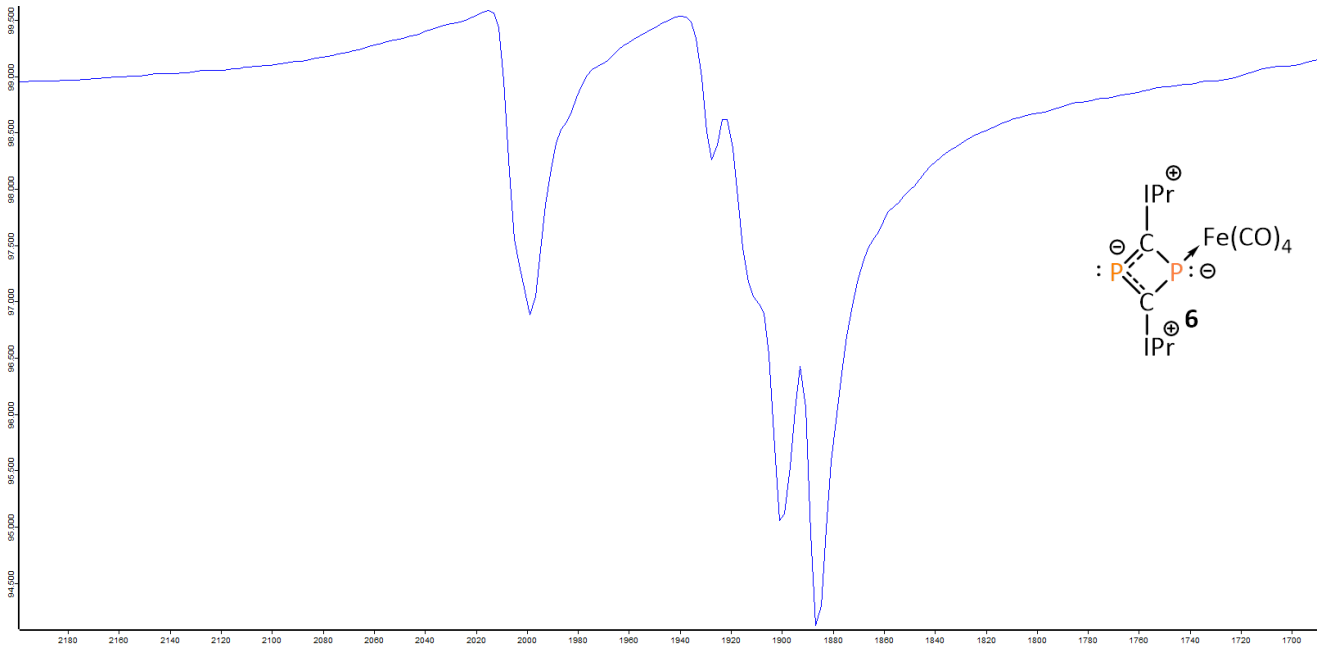

Figure S9: CO-region of the transmission-IR spectrum of **6** at room temperature in saturated n-hexane solution.

2. Calculations

2.1 General considerations

All calculations were carried out with the ORCA program package.[1, 2] Unless stated otherwise, all calculations were carried out on isolated molecules. Density fitting techniques, also called resolution-of-identity approximation (RI),[3] were used for GGA and *meta*-GGA calculations. Atom-pairwise dispersion corrections with the Becke-Johnson damping (D3BJ)[4, 5] were used for all DFT calculations. Orbital pictures were rendered with the software Chimaera.[6] All geometries and frequencies were obtained using the B97-3c method developed by the Grimme group[7]. EDA-NOCV calculations[8] were conducted using the TPSS[9] functional and the def2-TZVP[10] basis set.

2.2 **Results**

As indicated by their different tau values, **5** and **6** adopt different coordination environments around the iron centers. Here, **6** is closer to a trigonal-bipyramid and **5** is closer to a square-pyramid. Interestingly, calculations on small model complexes predict a preference of both ligands to support a trigonal-bipyramidal geometry around Fe. Thus, the bulky Ter and Dipp substituents in **5** and **6** are likely the cause for their different coordination geometries.

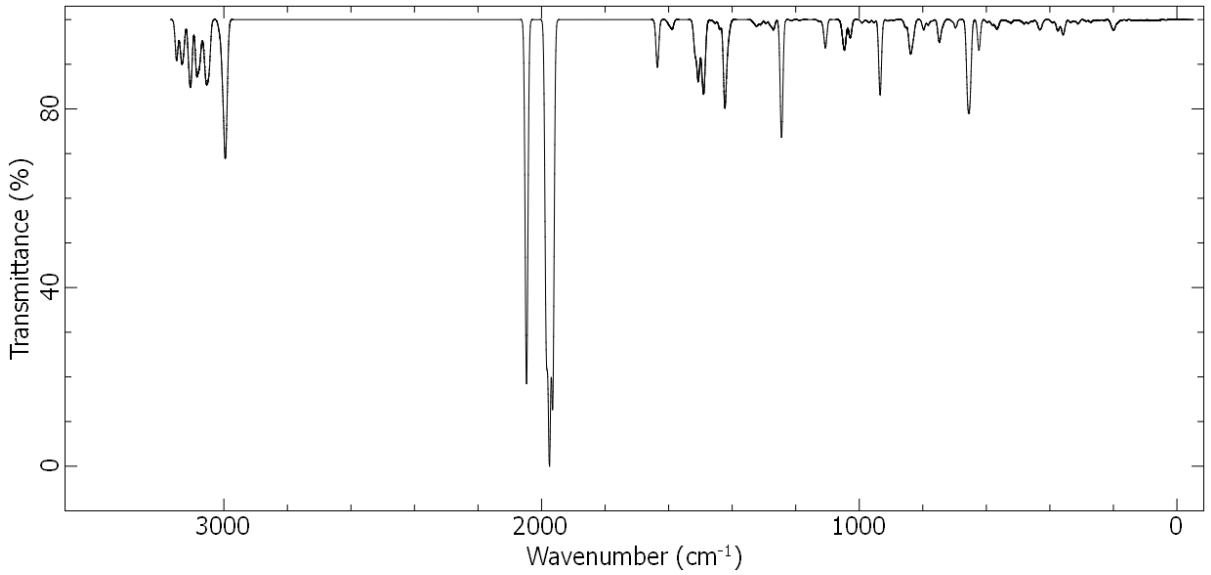

Figure S10: Simulated IR spectrum of **5**. CO-stretch frequencies are at 1965, 1975, 1985 and 2047 cm^{-1}.

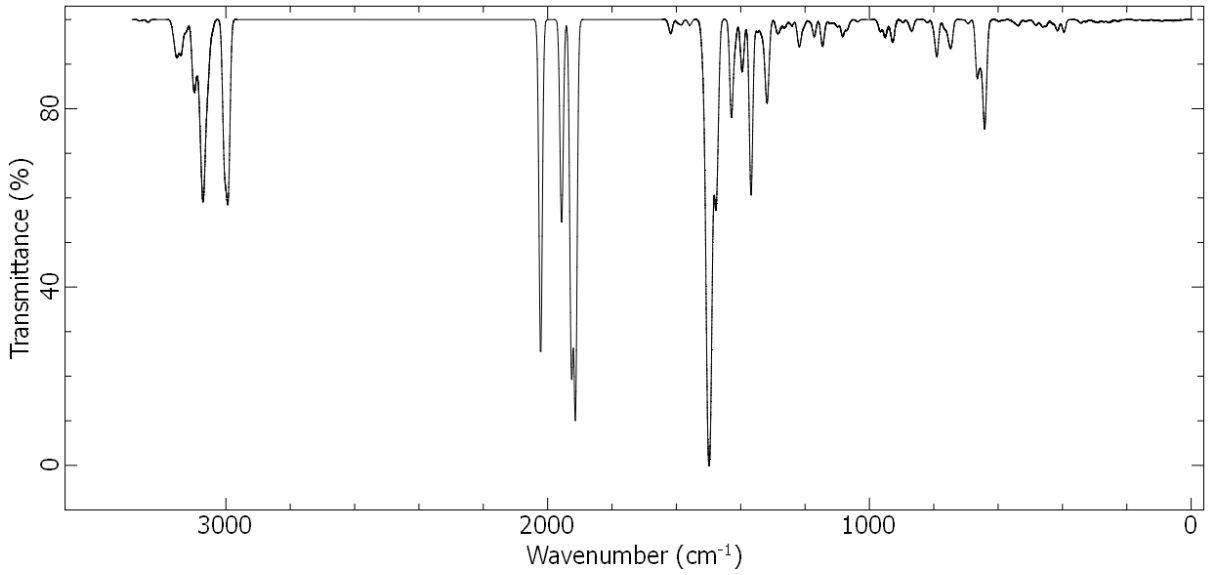

Figure S11: Simulated IR spectrum of **6**. CO-stretch frequencies are at 1913, 1926, 1957 and 2022 cm^{-1}.

EDA-NOCV calculations were carried out to get a deeper insight into the Fe-L interactions in **5** and **6**. Both, IDP and [P(μ-NTer)]$_2$ act as strong σ-donor and weak π-acceptor ligands in the tetracarbonyl complexes (see Figure S12 for a graphical representation). Thereby, in agreement with the conclusions drawn from IR-spectroscopy, IDP is a stronger σ-donor (68.3 vs. 50.6 kcal·mol^{-1}) and weaker π-acceptor (6.5 vs. 13.6 kcal·mol^{-1}) than [P(μ-NTer)]$_2$.

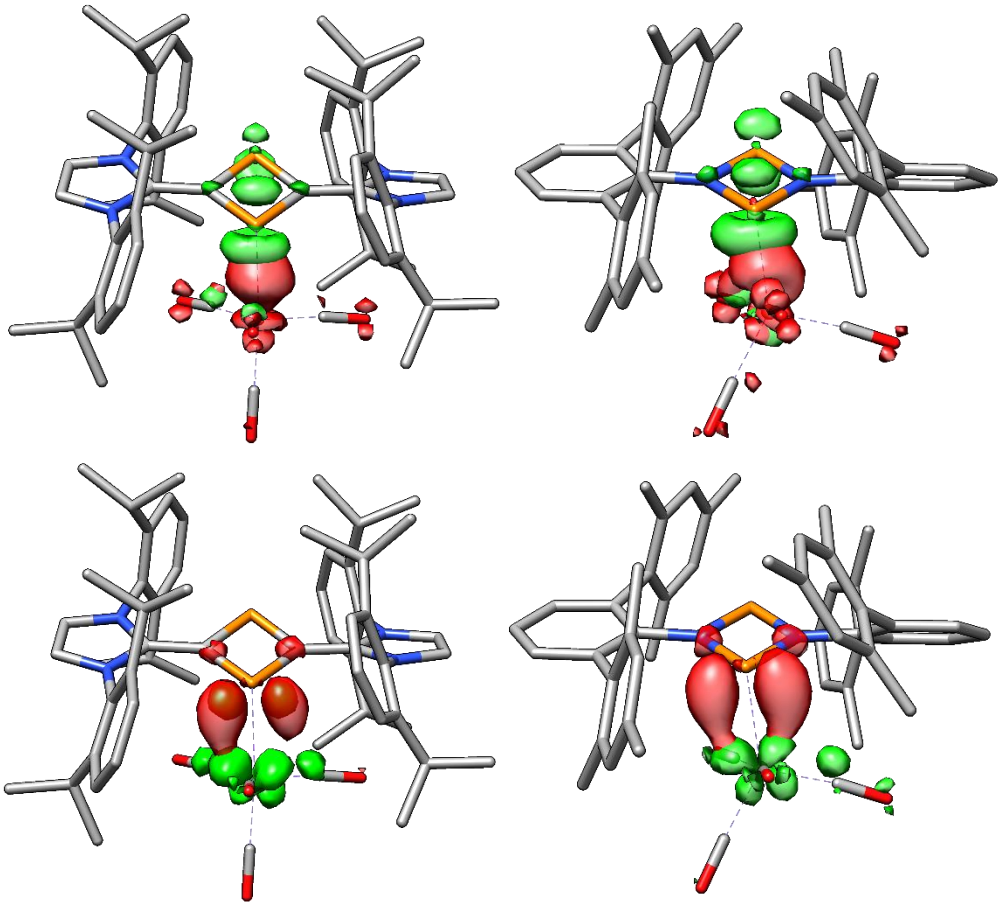

Figure S12: Metal-ligand interaction in **5** and **6**.

3. Crystallographic data

3.1 General considerations

Single crystals suitable for X-ray diffraction were coated with poly*iso*butylene oil in a glovebox, transferred to a nylon loop and then transferred to the goniometer of a Bruker X8 APEX2 or Bruker D8-Venture, equipped with a molybdenum (λ = 0.71073 Å) X-ray tube. Preliminary data was collected to determine the crystal system. The space group was identified and the data were processed using the Bruker SAINT+ program and corrected for absorption using SADABS. The structures were solved using direct methods (SHELXS[11]) on OLEX2[12] completed by Fourier synthesis and refined by full-matrix least squares.

3.2 Results

3.2.1 $[Fe(CO)_4$-$\{[P(\mu$-NTer$)]_2\}]$ (**5**)

Table S1: Crystallographic data for $[Fe(CO)_4$-$\{[P(\mu$-NTer$)]_2\}]$ (**5**)

Property	$[Fe(CO)_4$-$\{[P(\mu$-NTer$)]_2\}]$ (**5**)
Identification code	MS146
Empirical formula	$C_{52}H_{50}FeN_2O_4P_2$
Formula weight	884.73
Temperature[K]	99.99(11)
Crystal system	monoclinic
Space group	$P2_1/c$
a[Å]	11.5145(3)
b[Å]	19.2751(5)
c[Å]	20.6856(6)
α[°]	90
β[°]	105.083(3)
γ[°]	90
Volume[$Å^3$]	4432.9(2)
Z	4
ρcalcg[cm^3]	1.326
μ[mm^{-1}]	0.461
F(000)	1856.0
Crystal size[mm^3]	1 × 0.4 × 0.25
Radiation	Mo Kα (λ = 0.71073)
2Θ range for data collection[°]	3.664 to 56.564
Index ranges	-15 ≤ h ≤ 15, -16 ≤ k ≤ 25, -26 ≤ l ≤ 27
Reflections collected	19598
Independent reflections	10683 [R_{int} = 0.0224, R_{sigma} = 0.0400]
Data/restraints/parameters	10683/0/562
Goodness-of-fit on F^2	1.020
Final R indexes [I>=2σ (I)]	R_1 = 0.0384, wR_2 = 0.0916
Final R indexes [all data]	R_1 = 0.0488, wR_2 = 0.0970
Largest diff. peak/hole [e·$Å^{-3}$]	0.38/-0.35
CCDC Deposition Number	2093150

Table S2: Bond lengths of $[Fe(CO)_4$-$\{[P(\mu\text{-}NTer)]_2\}]$ (**5**).

bond		[Å] (**5**)	bond		[Å] (**5**)
Fe1	P2	2.2657(5)	C38	C39	1.506(2)
Fe1	C27	1.7751(19)	C31	C32	1.409(2)
Fe1	C26	1.8058(19)	C2	C1	1.412(2)
Fe1	C25	1.7961(17)	C2	C12	1.395(2)
Fe1	C28	1.782(2)	C1	C15	1.412(2)
P2	N1	1.7971(14)	C16	C15	1.501(2)
P2	N2	1.7748(14)	C16	C17	1.401(2)
P1	N1	1.6806(14)	C16	C23	1.407(2)
P1	N2	1.6639(14)	C32	C34	1.392(2)
O4	C25	1.147(2)	C32	C33	1.507(2)
O3	C26	1.147(2)	C37	C35	1.386(3)
N1	C29	1.4254(19)	C15	C14	1.390(2)
O2	C27	1.149(2)	C45	C47	1.392(2)
O1	C28	1.148(2)	C45	C46	1.506(2)
N2	C1	1.422(2)	C9	C7	1.384(3)
C29	C43	1.411(2)	C7	C6	1.388(3)
C29	C30	1.414(2)	C7	C8	1.515(2)
C44	C43	1.496(2)	C17	C19	1.390(2)
C44	C51	1.412(2)	C17	C18	1.504(2)
C44	C45	1.407(2)	C6	C4	1.392(2)
C43	C42	1.395(2)	C4	C5	1.506(3)
C30	C31	1.493(2)	C19	C20	1.389(3)
C30	C40	1.395(2)	C34	C35	1.387(3)
C51	C52	1.507(2)	C12	C13	1.385(2)
C51	C50	1.388(2)	C35	C36	1.505(3)
C3	C10	1.406(2)	C13	C14	1.381(3)
C3	C2	1.504(2)	C50	C48	1.392(3)
C3	C4	1.407(2)	C23	C22	1.393(2)
C10	C9	1.394(2)	C23	C24	1.508(3)
C10	C11	1.511(2)	C20	C22	1.386(3)
C41	C40	1.382(2)	C20	C21	1.507(3)
C41	C42	1.382(2)	C48	C47	1.387(3)
C38	C31	1.404(2)	C48	C49	1.510(3)
C38	C37	1.391(2)			

3.2.2 [$Fe(CO)_4$-{IDP}] (**6**)

Table S3: Crystallographic data for [$Fe(CO)_4$-{IDP}] (**6**).

Property	[$Fe(CO)_4$-{IDP}] (**6**)
Identification code	MS134_2
Empirical formula	$C_{60}H_{72}FeN_4O_4P_2$
Formula weight	1031.00
Temperature[K]	100.0
Crystal system	monoclinic
Space group	$P2_1/n$
a[Å]	10.5888(4)
b[Å]	28.1904(12)
c[Å]	18.7213(9)
α[°]	90
β[°]	95.400(2)
γ[°]	90
Volume[$Å^3$]	5563.6(4)
Z	4
ρcalcg[cm^3]	1.231
μ[mm^{-1}]	0.378
F(000)	2192.0
Crystal size[mm^3]	0.15 × 0.13 × 0.08
Radiation	MoKα (λ = 0.71073)
2Θ range for data collection[°]	4.494 to 54.206
Index ranges	−13 ≤ h ≤ 13, −36 ≤ k ≤ 36, −23 ≤ l ≤ 23
Reflections collected	65530
Independent reflections	12270 [R_{int} = 0.0920, R_{sigma} = 0.0661]
Data/restraints/parameters	12270/0/656
Goodness-of-fit on F^2	1.011
Final R indexes [I>=2σ (I)]	R_1 = 0.0480, wR_2 = 0.0936
Final R indexes [all data]	R_1 = 0.0869, wR_2 = 0.1089
Largest diff. peak/hole [e·$Å^{-3}$]	0.86/−0.45
CCDC Deposition Number	2093151

Table S4: *Bond lengths of [Fe(CO)$_4$-{IDP}] (**6**).*

bond		[Å] (**6**)	bond		[Å] (**6**)
Fe1	P2	2.3648(7)	C7	C6	1.520(3)
Fe1	C30	1.784(3)	C7	C8	1.520(4)
Fe1	C29	1.773(3)	C7	C9	1.533(4)
Fe1	C32	1.765(3)	C4	C3	1.337(4)
Fe1	C31	1.804(3)	C6	C10	1.393(4)
P2	P1	2.6824(9)	C57	C58	1.519(3)
P2	C33	1.824(2)	C57	C56	1.392(4)
P2	C1	1.820(2)	C38	C42	1.396(4)
P1	C33	1.764(3)	C38	C39	1.530(3)
P1	C1	1.745(2)	C50	C54	1.394(3)
O1	C30	1.159(3)	C50	C52	1.517(3)
O4	C29	1.158(3)	C17	C25	1.401(3)
O3	C32	1.159(3)	C17	C18	1.399(3)
N2	C37	1.453(3)	C25	C24	1.393(3)
N2	C34	1.379(3)	C25	C26	1.511(3)
N2	C36	1.397(3)	C58	C59	1.523(4)
N4	C2	1.377(3)	C58	C60	1.519(4)
N4	C5	1.446(3)	C14	C13	1.513(4)
N4	C4	1.393(3)	C14	C16	1.539(3)
N3	C2	1.374(3)	C14	C15	1.529(4)
N3	C17	1.446(3)	C13	C12	1.394(4)
N3	C3	1.384(3)	C24	C23	1.381(4)
N1	C34	1.383(3)	C54	C55	1.384(4)
N1	C49	1.444(3)	C18	C22	1.393(4)
N1	C35	1.384(3)	C18	C19	1.521(4)
O2	C31	1.143(3)	C22	C23	1.380(4)
C2	C1	1.409(3)	C52	C53	1.524(4)
C5	C6	1.397(3)	C52	C51	1.523(4)
C5	C13	1.405(3)	C43	C44	1.384(4)
C37	C45	1.404(3)	C43	C42	1.381(4)
C37	C38	1.399(3)	C55	C56	1.381(4)
C34	C33	1.398(3)	C26	C28	1.525(4)
C49	C57	1.402(3)	C26	C27	1.540(4)
C49	C50	1.394(3)	C10	C11	1.382(4)
C46	C45	1.521(3)	C11	C12	1.381(4)
C46	C47	1.522(3)	C39	C40	1.535(4)
C46	C48	1.534(3)	C39	C41	1.538(4)
C35	C36	1.337(3)	C19	C20	1.531(4)
C45	C44	1.392(3)	C19	C21	1.524(4)

3.3 Comparison of selected bond lengths

Table S5: Selected analytical data for **5**, **6**, **X** and $Fe(CO)_5$. Transmission-IR CO-stretching frequencies [cm^{-1}] are reported from n- hexane solution. ax. = axial, eq. = equatorial. Distances of the coordinated and non-coordinated ring-E atoms and structure coefficient τ_5[13] are compared. E = P for **5**, **6**; E = As for **X**.

Compound	CO-stretch freq. [cm^{-1}] in *n*-hexane solution	CO-stretch freq. [cm^{-1}] calculated	C-O-distance [Å]	(Fe)E^--C/N distance) [Å]	E^+-C/N distance [Å]	τ_5[13]
5	2034, 1967, 1949	2047, 1985, 1975, 1965	1.149(2)(ax.), 1.147(2)(eq.), 1.147(2) (eq.), 1.148(2) (eq.) Ø 1.148(2)	1.775(1), 1.797(1) Ø 1.786(1)[a]	1.664(1), 1.681(1) Ø 1.673(1)[b]	0.32
6	2001, 1928, 1900, 1886	2022, 1957, 1926, 1913	1.159(3)(ax.), 1.159(3)(eq.), 1.143(3) (eq.), 1.158(3) (eq.) Ø 1.155(3)	1.820(2), 1.824(2) Ø 1.822(2)[c]	1.745(2), 1.764(3) Ø 1.755(3)[d]	0.76
X[14]	–	–	1.163(5)(ax.), 1.156(4)(eq.), 1.148(5) (eq.), 1.154(5) (eq.) Ø 1.156(5)	1.964(3), 1.960(3) Ø 1.962(3)[e]	1.871(3), 1.881(3) Ø 1.876(3)[f]	0.76
$[Fe(CO)_5]$	2022, 2000[15]	–	1.117(2)(ax.), 1.136(2)(eq.), 1.128(2)(eq.) Ø 1.127(2)[16]	–	–	0.96[16]

[a]: P2−N1/2 distances; [b]: P1−N1/2 distances; [c]: P2−C1/3 distances; [d]: P1−C1/3 distances; [e]: As(Fe)−C distances; [f]: As−C distances.

4 References

1. Neese, F.W. F.; Becker, U.; Riplinger, C. *J. Chem. Phys.* **2020**, *152*, 224108, https://doi.org/10.1063/5.0004608.
2. Neese, F. *WIREs Computational Molecular Science* **2017**, *8*, https://doi.org/10.1002/wcms.1327
3. Kendall, R. A.; Früchtl, H. A. *Theor. Chem. Acc.* **1997**, 158–163
4. Grimme, S.; Antony, J.; Ehrlich, S.; Krieg, H. *J. Chem. Phys.* **2010**, *132*, 154104, https://doi.org/10.1063/1.3382344
5. Grimme, S.; Ehrlich, S.; Goerigk, L. *J. Comput. Chem.* **2011**, *32*, 1456–1465, 10.1002/jcc.21759.
6. Pettersen, E. F.; Goddard, T. D.; Huang, C. C.; Couch, G. S.; Greenblatt, D. M.; Meng, E. C.; Ferrin, T. E. *J. Comput. Chem.* **2004**, *25*, 1605–1612, https://doi.org/10.1002/jcc.20084.
7. Brandenburg, J. G.; Bannwarth, C.; Hansen, A.; Grimme, S. *J. Chem. Phys.* **2018**, *148*, 064104, https://doi.org/10.1063/1.5012601.
8. Mitoraj, M. P.; Michalak, A.; Ziegler, T. *J. Chem. Theory Comput.* **2009**, *5*, 962-975, https://doi.org/10.1021/ct800503d.
9. Tao, J.; Perdew, J. P.; Staroverov, V. N.; Scuseria, G. E. *Phys. Rev. Lett.* **2003**, https://doi.org/10.1103/PhysRevLett.91.146401.
10. Weigend, F.; Ahlrichs, R. *Phys. Chem. Chem. Phys.* **2005**, *7*, 3297–3305, https://doi.org/10.1039/B508541A.
11. Sheldrick, G. M. *Acta Cryst. A* **2008**, *64*, 112-122, https://doi.org/10.1107/S0108767307043930.
12. Dolomanov, O. V.; Bourhis, L. J.; Gildea, R. J.; Howard, J. A. K.; Puschmann, H. *J. Appl. Cryst.* **2009**, *42*, 339-341, https://doi.org/10.1107/s0021889808042726.
13. Addison, A. W.; Rao, T. N.; Reedijk, J.; van Rijn, J.; Verschoor, G. C. *Dalton Trans.* **1984**, , 1349-1356, https://doi.org/10.1039/dt9840001349.
14. Steffenfauseweh, H.; Vishnevskiy, Y. V.; Neumann, B.; Stammler, H.-G.; Andrada, D. M.; Ghadwal, R. *Angew. Chem. Int. Ed.* **2022**, *n/a*, https://doi.org/10.1002/anie.202207415.
15. Bigorgne, M. *J. Organomet. Chem.* **1970**, *24*, 211-229, https://doi.org/doi.org/10.1016/S0022-328X(00)91582-1.
16. Braga, D.; Grepioni, F.; Orpen, A. G. *Organometallics* **1993**, *12*, 1481-1483, https://doi.org/10.1021/om00028a082.

Author Contributions

M. T. Scharnhölz: Synthesis and analysis of all compounds, author of the original manuscript.
Dr. P. Coburger: Calculations, support in preparation of the manuscript, partial experimental work in development of the new route to **1**.
H. Beer: Preparation of **1**, development of new protocol for **1**, support in preparation of the manuscript.
Dr. J. Bresien: Administration of the project, support in preparation of the manuscript.
Prof. Dr. A. Schulz: Administration of the project, PI of H. Beer and J. Bresien
Prof. Dr. H. Grützmacher: Administration of the project, funding acquisition, preparation of manuscript, PI of M. T. Scharnhölz, Dr. P. Coburger.